Journal of Power Sources 222 (2013) 135–139

Contents lists available at SciVerse ScienceDirect

Journal of Power Sources

journal homepage: www.elsevier.com/locate/jpowsour

Short communication

Nanoporous Cu film/Cu plate with superior catalytic performance toward electro-oxidation of hydrazine

Falong Jia*, Jinhu Zhao, Xinxing Yu

College of Chemistry, Central China Normal University, Wuhan 430079, PR China

HIGHLIGHTS

- Nanoporous Cu formed by LSV dealloying of surface Cu–Zn alloy in short time.
- Lower onset oxidation potential of hydrazine on nanoporous Cu than smooth Cu.
- Superior activity of nanoporous Cu toward oxidation of hydrazine.
- Higher stability of nanoporous Cu than Cu nanoparticles.

GRAPHICAL ABSTRACT

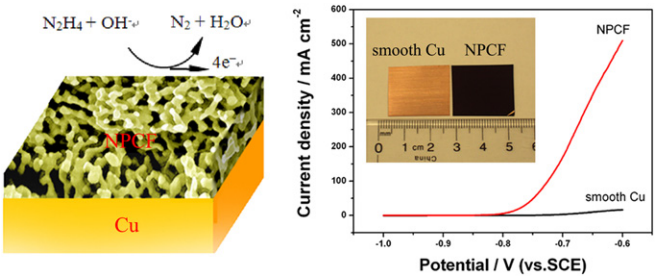

ARTICLE INFO

Article history:
Received 7 July 2012
Received in revised form
26 August 2012
Accepted 27 August 2012
Available online 5 September 2012

Keywords:
Copper
Fuel cell materials
Catalysis
Hydrazine

ABSTRACT

Nanoporous Cu film (NPCF) is fabricated on Cu plate by a novel electrochemical dealloying process in dilute HCl solution. The as-synthesized low-cost NPCF/Cu is used as anode in electro-oxidation of hydrazine for the first time and exhibits superior catalytic activity. The current density from hydrazine oxidation on NPCF is much higher than that on smooth copper. In addition, the NPCF electrode shows unexpected higher stability than Cu nanoparticles in similar size. It is believed that this low-cost NPCF electrode possesses potential application in the hydrazine fuel cell or other catalytic fields.

1. Introduction

Hydrazine has been considered as a candidate of fuels for fuel cells due to its high energy density. Compared with other conventional fuel cells, the direct hydrazine–air fuel cell (DHFC) has the following advantages [1]: (1) higher theoretical electromotive force of hydrazine cell (1.61 V) than conventional methanol–air fuel cells (1.21 V), (2) higher energy density of hydrazine fuel cell (5400 Wh L^{-1}) than that of methanol fuel cell (4820 Wh L^{-1}), (3) near ambient working temperature. The total reaction of hydrazine fuel cell can be written as [2]:

$$N_2H_4 + O_2 \rightarrow N_2 + 2H_2O \quad (1)$$

In alkaline solution, the electro-oxidation of N_2H_4 could be realized by the following reaction:

$$N_2H_4 + 4OH^- \rightarrow N_2 + 4H_2O + 4e^- \quad E^o = 0.84\,V \quad (2)$$

However, there are still some problems to be solved before its marketization. One of the key challenges is the development of low-cost catalysts for the hydrazine oxidation with superior catalytic activity as well as stability. By now, electro-oxidation of

* Corresponding author. Tel./fax: +86 27 67867953.
E-mail address: fljia@mail.ccnu.edu.cn (F. Jia).

0378-7753/$ – see front matter © 2012 Elsevier B.V. All rights reserved.
http://dx.doi.org/10.1016/j.jpowsour.2012.08.076

hydrazine had been investigated on various metals such as gold [3] and palladium [4]. Although noble metals exhibited satisfied catalytic performance and stability, their expensive cost still hindered the application of DHFC. Therefore, development of noble-metal free catalysts is highly desirable and important.

In the field of catalysis, metal nanoparticles normally exhibited superior performance than bulk materials due to their large surface-to-volume ratio and small-size effect, indicating a potential solution for the development of optimum catalysts for DHFC. Although copper nanoparticles were successfully used as catalysts in some organic reactions [5], its application in DHFC was seldom reported. Considering the practical use, Cu nanoparticles should be loaded on conductive substrates through adsorption method. There was a potential risk for these nanomaterials falling off during the long-term working, which would lead to the decrease of activation area. To avoid this problem, nanoporous copper as a whole integration could be a feasible solution. Among the ways to prepare nanoporous copper, dealloying process provided effective routes, which was involved with the selective dissolution of less noble elements from alloys (e.g. Cu–Mn, Cu–Al) [6,7]. Although dealloying of Zn from CuZn alloy is a well known phenomena in the field of corrosion [8], it was seldom reported that bulk Cu–Zn alloy was used to fabricate porous copper. The reason could be that the potential difference between Cu/Cu^{2+} and Zn/Zn^{2+} was not high enough to protect active nano-scaled Cu from corrosion during the etching of Zn. With dealloying process carried on from surface into deep area, the initially formed Cu tended to be corroded due to long exposure to etching solution.

The choice of solutions and dealloying parameters were also important in the fabrication processes. In our previous work, a thin film of nanoporous Cu was formed directly on the Cu plate by chemical dealloying of surface Cu–Zn alloy in alkaline solution [9]. However, it was found that over-corrosion of Cu always existed in the nanoporous film and part of NPCF tended to peel off from the plate. In this work, we chose electrochemical dealloying method to fabricate NPCF on Cu substrate and dealloying process could be finished in short time (<1 h). With precise control of potential applied on the sample, the corrosion speed could be well controlled and uniform nanoporous structure was obtained. The NPCF was found to be a good catalyst in the electro-oxidation of hydrazine (N_2H_4) and showed superior stability. It is believed that this NPCF/Cu electrode has a potential application in fuel cell device with hydrazine as energy source.

2. Experimental section

2.1. Preparation of NPCF electrodes

Copper plates (Sinopharm Chemical, 99.99%) were cleaned in acetone and then dipped into solution of 50 g L^{-1} $(NH_4)_2S_2O_8$ and 5 g L^{-1} H_2SO_4 for 30 s to remove oxide film. Then Zn was electrodeposited onto copper (0.5 cm^2 exposed area) at 20 mA cm^{-2} for 5 min from a commercial Zn plating solution (Fengfan Plating Corp.) [9]. Then, Cu–Zn sample was rinsed, dried and heated at 150 °C for 1 h under protection of N_2 gas. Finally, electrochemical dealloying of Cu–Zn sample was conducted through linear sweep voltammetry (LSV) by using a CHI660D electrochemical workstation. The applied potential was scanning from −1.0 V to −0.2 V at speed of 0.5 mV s^{-1}. Platinum plate, saturated calomel electrode (SCE) and Cu–Zn sample were used as reference electrode, counter electrode and working electrode, respectively.

2.2. Characterization and measurements

The microstructure and composition of the samples was characterized by field emission scanning electron microscopy (FESEM; JEOL-6700F) and energy dispersive X-ray Spectrometer (EDS; Oxford INCA.). X-ray diffraction (XRD) patterns of dealloyed Cu–Zn sample were recorded on a Rigaku diffractometer using Cu Kα radiation ($\lambda = 1.5418$ Å). The electrochemical oxidation of N_2H_4 was carried out in solution with 3 M NaOH and 1 M N_2H_4. The NPCF electrode, graphite plate and SCE were used as working electrode, counter electrode, and reference electrode, respectively. Smooth Cu working electrode was polished by aluminum oxide powder (~20 nm) before measurement. As for the test of Cu nanoparticles, 8 mg powder of Cu nanoparticles (~ 50 nm, Beijing Dk Nano technology Corp.) was dispersed in 1 ml AS-4 ionomer (Tokuyama Corp., Japan) suspension (5 wt.% in *n*-propanol) under ultrasonic condition and 5 μl of mixture was dropped onto glass-carbon electrode as working electrode.

3. Results and discussion

Fig. 1 shows the cross-sectional SEM images and components analysis of Cu–Zn samples. The thickness of deposited pure Zn layer was about 2.6 μm. After thermal treatment, some Zn remained as elementary substance on the top while a certain amount of Zn diffused into the Cu substrate. The atomic ratio of Cu increased gradually until the depth of film reached the pure Cu substrate. These results demonstrated that thermal treatment was an efficient way to form surface Cu–Zn alloy on Cu substrate.

Electrochemical dealloying of Cu–Zn sample was conducted in dilute HCl solution through linear sweep voltammetry (LSV) and results were listed in Fig. 2a. As for the Cu–Zn sample without thermal treatment, there was one anodic peak at potential ranging from −1.0 V to −0.77 V, which corresponded to the stripping of pure Zn. Since Cu substrate started to be oxidized at potential higher than −0.2 V, the ending potential of LSV was set as −0.2 V. After

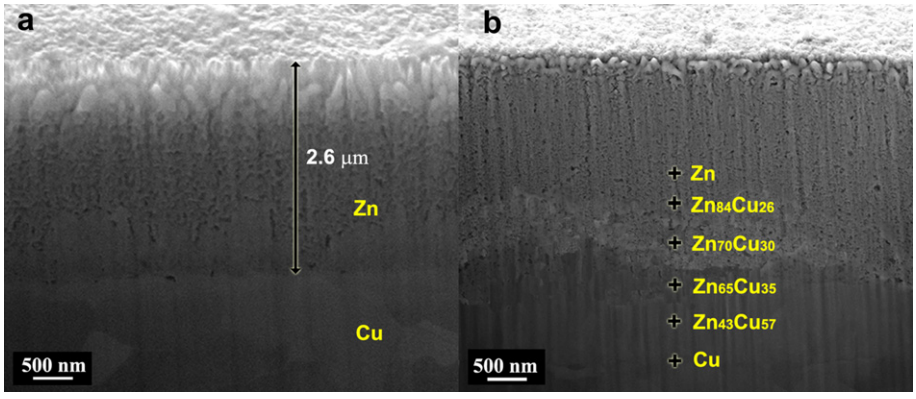

Fig. 1. Cross-sectional SEM images of Cu–Zn samples before (a) and after (b) thermal treatment.

thermal treatment, the first anodic peak resulted from stripping of pure Zn weakened and another two anodic peaks appeared at potential of −0.34 V and −0.23 V. These two peaks should be ascribed to the oxidation of Cu–Zn alloy layer since the electrochemical dealloying of Zn from Cu–Zn alloy was more difficult than pure Zn. SEM characterization results showed that porous structure was formed on the Cu substrate after LSV dealloying (Fig. 2b). There were voids in size of several hundred nanometers distributed on the rough surface. The magnified image revealed the existence of fine nanoporous structure with the ligament size of ∼40 nm (Fig. 2c).

The morphologies of samples were closely related with the parameters of electrochemical dealloying. When the electrochemical dealloying was conducted at constant potential of −0.2 V, the dissolution behavior of Zn was quite different from that in LSV process. As shown in Fig. 2d, the oxidation current was as high as 133 mA cm^{-2} initially and then decreased sharply to 1 mA cm^{-2} in 100 s. By contrast, the oxidation current increased slowly from zero at −1.0 V to 12 mA cm^{-2} at −0.87 V in 260 s (Fig. 2a). This result indicated that the dissolution of Zn under constant potential anodization was much faster than that in LSV process. After 800 s, the oxidation current decreased gradually to nearly zero and no more Zn was dissolved. The structure of as-synthesized film was more likely a kind of aggregation of irregular nanoparticles (Fig. 2e and f), which may cause negative effect on the surface area of the NPCF. During dealloying process, the residual Cu atoms would aggregate to form ligaments due to the tendency of surface-energy reduction. In the same time, pores and crevice were formed to balance the missing volume accompanying with the dissolution of Zn. Furthermore, rearrangement and self-organization of Cu atoms driven by surface diffusion would lead to formation of nanoporous structure. To fabricate fine nanoporous structure, it is important to control dissolution speed of Zn. If dissolution of Zn was finished in much shorter time such as that under constant potential anodization (Fig. 2d), there were few pores in the film and aggregation of residual Cu was in form of nanoparticles instead of ligaments (Fig. 2e and f). The reason could be that residual Cu would tend to aggregate together with lower surface area to compensate the fast vanishing volume caused by dissolution of Zn. Therefore, moderate dissolution of Zn by LSV dealloying would be helpful for residual Cu to reassemble into fine porous structure.

The composition of the nanoporous film was characterized by EDS analysis and small amount of Zn (∼8.5 at.%) still remained (Figure S1a). It was quite possible that the residual Zn existed in the status of alloy with Cu, which is more stable than pure Zn. X-ray diffraction (XRD) patterns of dealloyed Cu–Zn sample were recorded on a Rigaku diffractometer using Cu Kα radiation ($\lambda = 1.5418$ Å). Figure S1b shows that the strong peaks located at 43.4°, 50.6° and 74.3° are assigned to (111), (200) and (220) planes of Cu (JCPDS file No. 89-2838), respectively. Other weak peaks at 34.9°, 37.9°, 48.0° and 62.7° match well with the pattern of Cu_5Zn_8 (JCPDS file No. 71-397), proving that the residual Zn in the NPCF exists as Cu–Zn alloy. Comparing with electrochemical dealloying process, the dissolution of Zn usually took much longer time in chemical dealloying. According to our previous work in alkaline etching system, there were always cracks in the porous film (see Figure S2 in supporting file). Due to the existence of cracks, the nanoporous film was not stable and easy to peel off when slightly bending the Cu plate. Considering good integrity of NPCF/Cu was first important for its application as electrode, the NPCF/Cu prepared by chemical dealloying was not suitable to be used in DHFC. In contrast, the NPCF prepared by LSV dealloying was combined with Cu plate firmly and no peeling of film was observed after bending.

To investigate potential application of NPCF in the hydrazine fuel cell, the following experiments were carried out to investigate

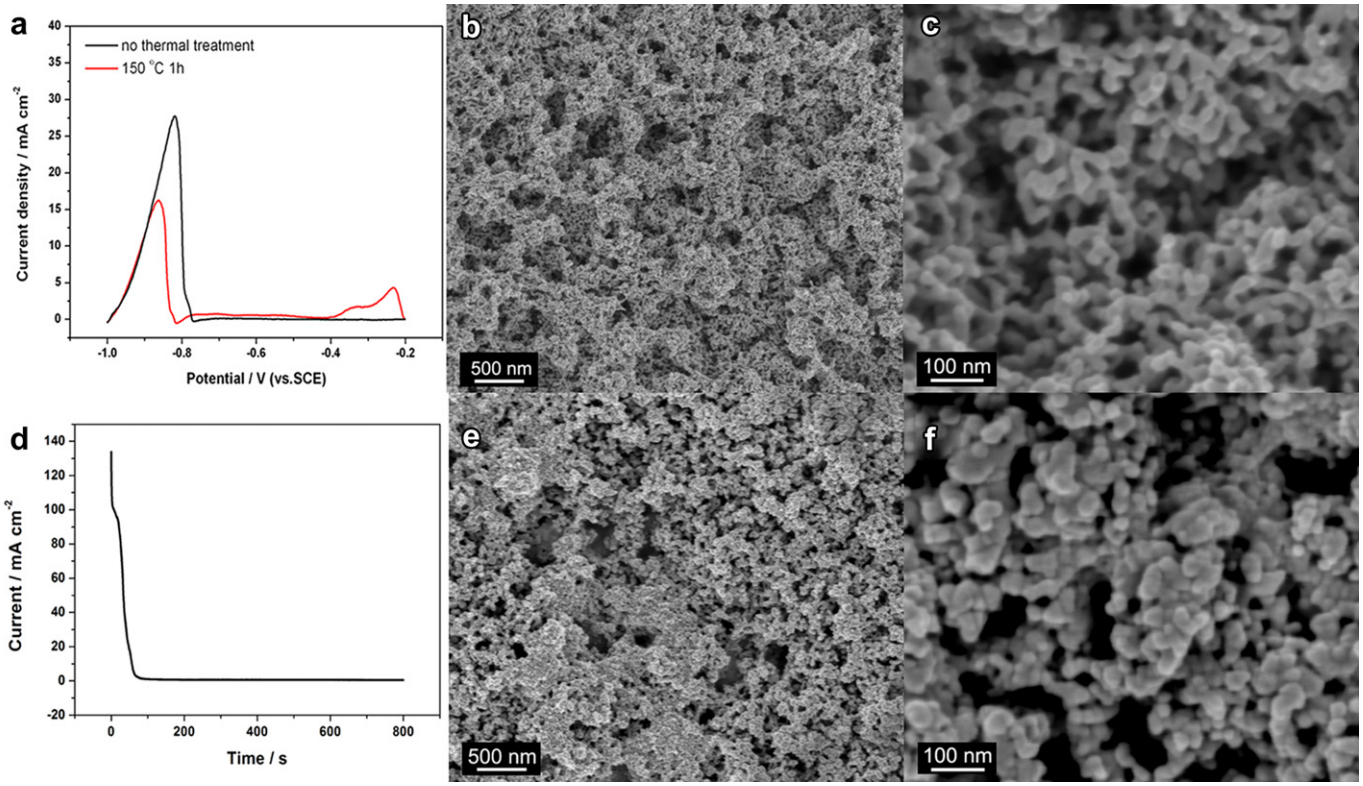

Fig. 2. (a) LSV curves of Cu–Zn samples at scan rate of 0.5 mV s^{-1}; (b, c) SEM images of sample after LSV dealloying; (d) Current–time curve recorded for dealloying at constant potential of −0.2 V (vs. SCE); (e, f) SEM images of sample after constant-potential dealloying.

its catalytic performance. Fig. 3a shows the electrochemical behavior of smooth Cu plate in the NaOH solution with and without hydrazine. From the LSV curve in the solution without hydrazine, it can be seen that the copper starts to be oxidized obviously at −0.55 V. In the solution with 0.5 M or 1 M hydrazine, there was always an anodic peak at potential of around −0.58 V in the LSV curve. This obvious anodic peak should be attributed to the oxidation of hydrazine since the current value at this peak was almost proportional to the concentration of hydrazine. Considering that copper could be oxidized at potential more positive than −0.55 V, the maximum potential in the following LSV was set at −0.6 V to prevent the negative effect of potential corrosion on the catalytic performance of NPCF. Fig. 3b gives a comparison of catalytic performance on electrodes of NPCF, smooth Cu and gold electrodes in the solution with same concentration of hydrazine. At the same potential of −0.6 V, no obvious current was observed on gold electrode while there was considerable current (16 mA cm^{-2}) on smooth Cu electrode. This result indicated that smooth Cu exhibited superior catalytic performance than gold toward the oxidation of hydrazine. After nanoporous film was formed on the Cu electrode, the anodic current density was improved greatly and almost 50 times higher than that on smooth Cu at −0.7 V. The onset oxidation potential (E_{on}) of hydrazine was usually regarded as evaluation criteria to compare the performances of catalysts [10]. Here, the E_{on} on NPCF (−0.87 V) was lower than that on smooth Cu plate (−0.77 V). The obvious 100 mV negative potential shift indicated that NPCF possessed better oxidation ability to the hydrazine and may work at more negative potential. To investigate the real reason for the enhancement of catalytic performance, Cu nanoparticles with similar size as that of ligament size in NPCF were tested in the same electrolyte. Results showed that E_{on} of hydrazine oxidation on Cu nanoparticles was around −0.89 V, suggesting that the lower E_{on} on NPCF could be ascribed to the nano-sized structure of NPCF.

As mentioned in above results, the morphologies of NPCF were affected greatly by dealloying processes, which may lead to the difference in the electrochemical activity. Fig. 4a shows the oxidation currents of hydrazine at −0.6 V on the electrodes of smooth Cu and NPCF/Cu samples prepared under different conditions. As for the smooth Cu, the current density is only 16 mA cm^{-2}. When constant potential (−0.2 V) was applied during dealloying, the produced NPCF/Cu exhibited higher current density 244 mA cm^{-2}. If NPCF/Cu was prepared through LSV process, the current density was improved further to 510 mA cm^{-2}. We also checked the performance of sample prepared through chemical dealloying referring to our previous work, the current density was 150 mA cm^{-2} lower than that of NPCF by LSV dealloying. The active surface area of Cu samples could be evaluated by the integration of charge consumed in the reduction of copper oxide, which was formed during the anodic scan in alkaline solution (Figure S3). Since the charge consumed in the reduction of copper oxide was proportional to the active surface area of copper electrode, it could be calculated that the surface area of NPCF/Cu by LSV dealloying was 22 times that of smooth Cu. By this way, the specific current density was obtained by normalization to the surface area of NPCF/Cu samples (considering the surface area of smooth Cu is approximately equal to the geometric area). In Fig. 4a, NPCF/Cu prepared by LSV dealloying possessed the highest specific current density, which was 38% higher than that of smooth Cu.

Besides specific activity, the stability is also another important property of electrode material. It had been reported that metal nanoparticles were not stable and the size distribution of nanoparticles tended to increase due to Oswald ripening [11,12]. Oswald ripening was a thermodynamically-driven phenomenon that smaller nanoparticles dissolved and re-deposited on larger particles, which led to the decrease of electrochemical activation area. To evaluate the stability of the NPCF electrode, continuous cyclic potential scan was applied onto the NPCF electrode and the current density at −0.6 V in each cycle was recorded. Fig. 4b shows the change of current density versus cycles of CV in hydrazine solution by use of NPCF. The current density gradually decreased to 90% of the original value in 30 cycles and remained stable in the following 70 cycles. But with copper nanoparticles as electrode material, the degradation of current density was faster and 74% of original value remained after 100 cycles. The results indicated the stability of NPCF was higher than independent Cu nanoparticles. The EDS analysis showed that atomic ratio of Zn in NPCF decreased to 3.1 at.% after the cycled test, which indicates that some part of Zn component was etched further in the hydrazine oxidation. However, the porous structure of NPCF changed little after 100 cycles (inset in Fig. 4b). The reason is probably that the special three-dimensional nanoporous structure could contribute partly to the maintenance of nanoporous structure. In our previous work, it was found that the three-dimensional nanostructured networks of platinum exhibited superior stability on the individual Pt nanoparticles on carbon support [13]. As a thermodynamic favorable structure, nanostructured networks may protect the structure from destroying by Ostwald ripening during the electrochemical process

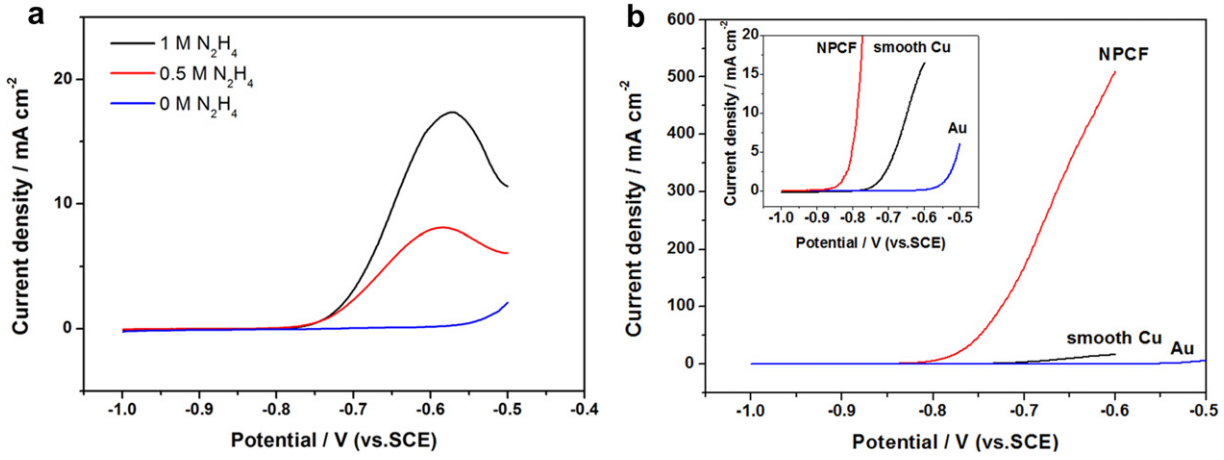

Fig. 3. (a) LSV curves of smooth Cu electrode in 3 M NaOH with 0 M, 0.5 M, and 1 M hydrazine; (b) LSV curves of electro-oxidation of hydrazine by use of NPCF/Cu (same as Fig. 2b), smooth Cu and gold electrodes. Inset picture is the corresponding magnified curves. The potential scan rate was 50 mV s^{-1}.

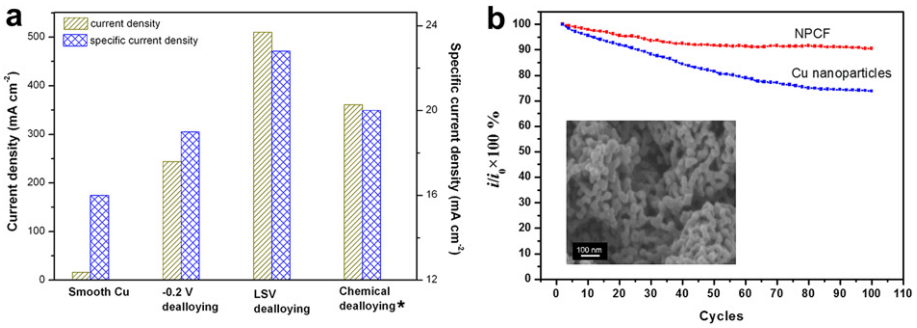

Fig. 4. (a) The oxidation current and specific current density (normalized to the surface area) of hydrazine at −0.6 V by the use of smooth Cu and different NPCF/Cu samples. Label * corresponds to the sample of Fig. 3c in Ref. [9]; (b) change of current at −0.6 V versus cycles of CV (−1.0 → −0.6 → −1.0 V) in hydrazine solution on the electrodes of NPCF (LSV dealloyed) and Cu nanoparticles. Inset picture is the SEM image of NPCF after 100 cycles.

[11]. There could be a similar mechanism here for the enhancement of stability of NPCF and detailed reason will be discussed in further report.

4. Conclusion

In summary, nanoporous copper film was successfully fabricated on copper substrate through electrochemical dealloying of annealed Cu–Zn sample in dilute HCl solution. Due to the uniform potential applied onto the surface of sample, the dissolution speed of Zn was well controlled to produce fine nanoporous structure. Primary results showed that the resulted NPCF/Cu electrodes possessed superior catalytic performance to the electro-oxidation of hydrazine than smooth copper plate. Among all the samples prepared by electrochemical or chemical dealloying methods, the highest oxidation current density of hydrazine was obtained on the NPCF/Cu sample fabricated by LSV in 25 mM HCl. Furthermore, the NPCF/Cu exhibited better stability than copper nanoparticles and its morphology changed little after 100 cycles of electro-oxidation of hydrazine. This special nanoporous copper material could be a promising candidate for anode in hydrazine fuel cell.

Acknowledgment

This work was supported by National Science Foundation of China (Grants 21073069, 21073070, and 91023010) and Self-determined research funds of CCNU from the colleges'basic research and operation of MOE (CCNU11A02006).

Appendix A. Supplementary data

Supplementary data related to this article can be found at http://dx.doi.org/10.1016/j.jpowsour.2012.08.076.

References

[1] H. Liu, J. Zhang, Electrocatalysis of Direct Methanol Fuel Cells, Wiley-Vch Verlag Gmbh & Co. KGaA, Weinheim, 2009, p. 528.
[2] N.V. Rees, R.G. Compton, Energy Environ. Sci. 4 (2011) 1255–1260.
[3] K. Kořínek, J. Koryta, M. Musilová, J. Electroanal. Chem. Interfac. 21 (1969) 319–327.
[4] B. Dong, B.-L. He, J. Huang, G.-Y. Gao, Z. Yang, H.-L. Li, J. Power Sources 175 (2008) 266–271.
[5] A. Sarkar, T. Mukherjee, S. Kapoor, J. Phys. Chem. C 112 (2008) 3334–3340.
[6] L.Y. Chen, J.S. Yu, T. Fujita, M.W. Chen, Adv. Funct. Mater. 19 (2009) 1221–1226.
[7] Z. Qi, C.C. Zhao, X.G. Wang, J.K. Lin, W. Shao, Z.H. Zhang, X.F. Bian, J. Phys. Chem. C 113 (2009) 6694–6698.
[8] Z.C. Liu, L.Y. Lin, S.F. Liu, Y.H. Zhao, Trans. Nonferrous Met. Soc. China 9 (1999) 572–577.
[9] F. Jia, C. Yu, K. Deng, L. Zhang, J. Phys. Chem. C 111 (2007) 8424–8431.
[10] A. Serov, C. Kwak, Appl. Catal. B: Environ. 98 (2010) 1–9.
[11] P.L. Redmond, A.J. Hallock, L.E. Brus, Nano Lett. 5 (2004) 131–135.
[12] Z. Chen, M. Waje, W. Li, Y. Yan, Angew. Chem. Int. Ed. 46 (2007) 4060–4063.
[13] F. Jia, F. Wang, Y. Lin, L. Zhang, Chem. Eur. J. 17 (2011) 14603–14610.